A Study of Compressible Turbulent Reattaching Free Shear Layers

M. Samimy*
Ohio State University, Columbus, Ohio
H. L. Petrie†
Pennsylvania State University, State College, Pennsylvania
and
A. L. Addy‡
University of Illinois, at Urbana-Champaign, Urbana, Illinois

An experimental investigation was conducted to study the two-dimensional, compressible, turbulent reattaching free shear layer formed by the geometrical separation of a Mach 2.46 flow with a turbulent boundary layer and a Reynolds number of 5.01×10^7/m from a 25.4 mm high backward-facing step. The wind tunnel test section was specifically designed to obtain a constant pressure separation at the step. A detailed survey of the flowfield was made utilizing a Schlieren system, static pressure taps, and a two-component coincident laser Doppler velocimeter. In contrast to incompressible reattaching free shear layers, significant increases in the turbulence level, shear stress, and turbulent triple products were observed within the reattachment region. Large turbulence structure and enhanced mixing were observed in the redeveloping region.

Nomenclature

M	= Mach number
p	= pressure
pr	= start of pressure rise
Pr	= turbulence production
r	= location of reattachment
u	= mean velocity in the streamwise direction
u^*	= Van Driest generalized velocity
u_τ	= friction velocity
x,y	= horizontal and vertical coordinates
$y_{0.5}$	= y component distance where $u = 0.5u_\infty$
δ	= boundary layer or shear layer thickness, where $u = 0.99u_\infty$
θ	= momentum thickness
ρ	= density
σ	= standard deviation with subscripts u or v
τ	= shear stress
$\langle\ \rangle$	= ensemble average

Superscripts

$\overline{(\ )}$	= mean value
$(\ )'$	= fluctuation from mean value

Subscripts

max	= maximum value
u	= streamwise
v	= transverse
w	= wall value
z	= spanwise
∞	= freestream value
0	= value of the boundary-layer parameter at the backstep and centerline value
0, 0.5, 0.99	= location where $u/u_\infty = 0$, 0.5, 0.99

Received Nov. 16, 1984; revision received March 18, 1985; presented as Paper 85-1646 at the AIAA 18th Fluid Dynamics, Plasmadynamics, and Lasers Conference, Cincinnati, OH, July 16-18, 1985.

*Assistant Professor, Department of Mechanical Engineering. Member AIAA.

†Research Associate, Applied Research Laboratory. Member AIAA.

‡Professor and Associate Head, Department of Mechanical and Industrial Engineering. Associate Fellow AIAA.

Introduction

AFTER many years of investigation, the problem of flow separation and subsequent flow recompression and redevelopment in the base region of a blunt based missile-type body still offers a great challenge to experimentalists and analytical and computational modelers. Since the early 1950s, analysis of separated flows for both laminar and turbulent supersonic base flows have been carried out along two paths, namely, the Chapman-Korst component model[1,2] and integral methods.[3,4] Although these methods are good engineering tools for analyzing base flow problems, they lack generality and leave unanswered many questions regarding the fundamental fluid dynamic nature of the flow mechanisms and interactions within the separated base flow region. This lack of knowledge is most apparent when an attempt is made to extend the models to more complex systems, geometries, and/or flight conditions.

The lack of understanding of the physics of the separated flows and the lack of reliable experimental data have slowed progress in the numerical modeling of this problem. Recent papers by Marvin,[5] Horstman et al.,[6] and Weinberg et al.[7] have shown good computational prediction of the separated flowfields with a small separated region but only a qualitative prediction with a large separated region, especially in the highly turbulent reattachment and redevelopment regions. The overall objectives of this study were to learn more about the fundamental nature of the recompression, reattachment, and redevelopment processes and to obtain some detailed data useful for analytical and computational modeling purposes.

Experimental Program

A series of dry, cold air experiments were conducted in a small-scale, blowdown wind tunnel facility.[8] The test section of the wind tunnel is shown in Fig. 1. The wind tunnel width was 50.8 mm and the step height was 25.4 mm. This configuration was specifically designed to eliminate the expansion effects at the separation point and provide a long constant-pressure free shear layer with a well-defined initial condition

to the compression and reattachment processes. The ramp angle was 19.4 deg, and the ramp leading apex distance from the step was 69.85 mm. Settles et al.,[9] Hayakawa et al.,[10] and Petrie et al.[11] have used configurations similar to that of the present study. Settles and Hayakawa used a hot-wire anemometer to survey the entire flowfield in a wind tunnel facility with a Mach 2.92 incoming flow with a turbulent boundary layer. Petrie used the laser Doppler velocimeter (LDV) to study only the constant-pressure region of the shear layer in a Mach 2.44 incoming flow with a turbulent boundary layer. Ikawa and Kubota[12] and Petrie et al.[11] also generated constant-pressure shear layers over a backward-facing step by using mass bleed from the floor of the wind tunnel. In their investigations, Ikawa and Kubota used a hot-wire anemometer and Petrie et al. used an LDV.

Information obtained from schlieren photographs, static pressure data, and LDV results were used to construct Fig. 1, and the regions of the flowfield with distinct features are identified for later discussion. The curves of $u=0$, $0.5u_\infty$, $0.99\mu_\infty$, and the sonic line, $M=1$, are shown. As can be seen, the $M=1$ and $u=0.5u_\infty$ locations were almost coincident. The station numbers where the vertical surveys of the flowfield were carried out are shown above the x axis in this figure.

The approach Mach number, Reynolds number, stagnation pressure, and stagnation temperature were 2.46, 5.01×10^7/m, 528.1 kPa, and 297 K, respectively. The approach boundary-layer and momentum thicknesses were 3.12 and 0.25 mm, respectively.

Laser Doppler Velocimetry Considerations

A two-color, two-component LDV system was utilized to make the velocity measurements. The frequency of one beam of each beam pair was shifted by 40 MHz in order to detect velocity direction and to eliminate fringe bias.[13-15] A 250 mm focal length lens was used for the velocity measurements within the boundary layer and the initial part of the shear layer, and a 600 mm focal length lens was used for the velocity measurements in the reattachment and redevelopment regions. The measurement volume diameter and length for the 250 and 600 mm lens were 0.131 and 1.83 mm and 0.314 and 4.39 mm, respectively. The 600 mm lens produced a large fringe spacing and a large fringe velocity in the measurement volume. These were desirable LDV system characteristics because of the high turbulence intensities expected in the reattachment and redevelopment regions[9] and possible fringe bias problems that may have resulted from the two-component coincident LDV.[8]

Seed particle generation was accomplished with a commercial six-jet atomizer. A 50 cP silicone oil was atomized and the effective mean diameter of the generated particles was estimated by measuring the relaxation of the velocity of particles downstream of an oblique shock wave.[16] The results indicated that the effective mean particle diameter was approximately 1 μm.

The individual velocity realization type data processor used in these experiments had the capability of measuring and storing 83.3 k coincident samples/s. The maximum data rate was approximately 2000 samples/s with the 250 mm lens and 400 samples/s with the 600 mm lens. Therefore, the sampling process was totally controlled by the flow. According to Erdmann and Tropea,[17,18] this "free-running" processor condition is completely velocity-biased. The two-dimensional velocity inverse weighting factor $|1/V_T|$ was used to correct for velocity bias, where V_T is the total velocity.

The digital frequency counters used in these experiments had a ±1 ns resolution. The maximum Doppler signal frequency was approximately 95 MHz, and the uncertainty due to counter clock resolution in a 5 to 8 frequency comparison could reach 3.1% at this frequency. Thus, the comparison level was set at 4% to avoid discarding data because of clock resolution.

In the separation region just downstream of the step, the velocity gradient across the shear layer was very large; therefore, errors in the velocity statistics due to spatial resolution were the largest. In this region, measurement errors due to spatial resolution were the largest and were estimated to be 0.9% in mean velocity and 1.9% in turbulence intensity.[19,20]

The data rate was approximately 2000 samples/s in the freestream and dropped to 20 samples/s in the recirculating region. The following number of samples were collected: 1024 in the freestream, 2048 in the recirculating region, and 4096 elsewhere. Therefore, the statistical uncertainty due to the limited sample size was estimated to be approximately $\pm3\%$ in the mean velocity and $\pm3.5\%$ in the turbulence intensity in the recirculating region. Elsewhere in the flowfield the statistical uncertainty was much lower.

Fringe bias occurs because the LDV frequency counters require a minimum number of fringes to be crossed before a signal is accepted.[13-15] Due to the highly turbulent nature of the flow in the present experiments, it was thought, at the outset, that fringe bias would be the major problem in designing these experiments. The fringe bias analysis of Buchhave[13] was modified to incorporate frequency shifting and was then used to correct for possible fringe bias.[8] The largest difference between the results that were corrected and uncorrected for fringe bias was 3%. Consequently, only the uncorrected results are presented herein.

Experimental Results

In this section, the experimental results are presented and compared to the results of previous studies. The nature of the incoming boundary layer, the pressure field, and the two-dimensionality of the flowfield are first discussed, and then the results for the mean flow and the turbulent flow are presented.

Incoming Boundary Layer

Two-component and one-component velocity measurements were made to within 1 and 0.25 mm of the wall, respectively. The approach boundary-layer and momentum thicknesses were determined to be 3.12 and 0.25 mm, respectively. The ratio of momentum thickness to boundary-layer thickness was 0.0792, which was approximately 10% higher than the value reported by Maise and McDonald.[21]

Maise and McDonald[21] defined a single curve, which was based on the wall-wake law coupled with the Van Driest compressibility transformation, and showed that they could collapse experimental data from numerous equilibrium-compressible boundary-layer flows. The maximum scatter of the data relative to their curve was approximately 30%. Figure 2 shows the boundary-layer data of the current study in comparison with the Maise and McDonald curve. The maximum difference between the present data and their curve is less than 5%; this is a good indication that the boundary layer of the

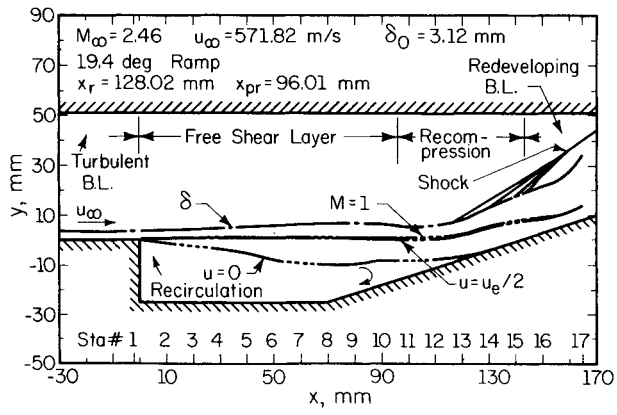

Fig. 1 Scaled map of the flowfield.

present study was in equilibrium. Since the skin-friction coefficient C_f was not measured directly, it was determined from the wall-wake law. The value of C_f determined by this method was 0.00138, which is in good agreement with the values of Refs. 9 and 11.

The boundary-layer shear stress profile is shown in Fig. 3. Also included in Fig. 3 are the incompressible results of Klebanoff,[22] the "best estimate" for the supersonic boundary-layer shear stress distribution given by Sandborn,[23] and the hot-wire and LDV data of Johnson and Rose[24] for a Mach 2.9 boundary-layer flow. The present data agree well with the LDV data of Johnson and Rose and with the best estimate of Sandborn up to $y/\delta = 0.8$, but in the upper edge of the boundary layer, the present data show somehow higher values.

Static Pressure Results

The wall pressure distribution nondimensionalized by static pressure before the step is shown in Fig. 4. The accuracy of the pressure measurements was approximately ±0.6%. The pressure change was less than 4% from 12.5 mm before separation to 96 mm after separation. The reattachment location, which was determined by coating the ramp surface with a steam engine oil-zinc oxide mixture, was located 128.02 mm downstream of the step and 4.91 mm vertically below a straight horizontal line extended from the step (see Fig. 4). At the last station, $x = 172.72$ mm, the pressure ratio was 2.83, which was significantly less than the final expected recovery pressure ratio of approximately 3.25. The experimental results of Roshko and Thomke,[25] Sirieix et al.,[26] and Settles et al.[9] have shown that the reattachment process is to a significant degree independent of the wall geometry or disturbances downstream of the reattachment location. Therefore, the relatively short length of the present ramp downstream of the reattachment location would be expected not to disturb the reattachment process during the current investigation.

Spanwise wall pressure distributions in three streamwise locations are shown in Fig. 5. As can be seen, the variations in the spanwise pressure distributions do not show any significant trends and are all within ±0.8% of the centerline pressure. Since the accuracy of the pressure measurements was determined to be ±0.6%, the flow was found to be two-dimensional within ±19 mm of the wind tunnel centerline.

Two Dimensionality of the Flowfield

Spanwise cellular structure has been noticed in the reattachment region using surface flow visualization.[16,25,27] This structure was also observed in the present experiments by coating the ramp surface with a steam engine oil-zinc oxide mixture. This structure was absent in the recent experimental study of Settles et al.[9] Thus, the existence of such spanwise motions is still a point of discussion and concern. Some detailed pressure measurements by Roshko and Thomke[25] have indicated that these secondary motions have very small effects on the static pressure distribution. The spanwise surface pressure distributions in two streamwise locations in the reattachment and redevelopment regions of the present study, which were discussed earlier and are shown in Fig. 5, are in agreement with the findings of Roshko and Thomke.[25]

Uniformity of the mean velocity and turbulence field across the tunnel in the reattachment and redevelopment regions was confirmed by LDV measurements made ±8.0 mm on either side of the centerline of the wind tunnel at $x = 130$ and 140 mm. The variation in data for the worst cases was ±2.1% in the mean velocity, ±2.8% in the streamwise turbulence intensity, and ±2.7% in the shear stress. Since the turbulence intensities and shear stress reached maximum values near $x = 140$ mm, these variations were within the statistical uncertainty of the finite sample sizes. LDV measurements further off-center were not possible due to reflections of laser light from the windows.

Based on the spanwise pressure measurements and off-center LDV measurements, it is concluded that the mean flowfield was uniform within a region ±19 mm of the centerline. From LDV measurements, the turbulence field was shown to be uniform within ±8.0 mm of the wind tunnel centerline.

Mean Flow Results

The mean velocity profiles for all stations are shown in Fig. 6. The abscissa shows the vertical station numbers, the dashed vertical lines show the locations of zero velocities for each station, and the number above the dashed lines show the x locations of the stations. The mean velocities were normalized by the approach freestream velocity $u_\infty = 571.82$ m/s. The variation in freestream velocity above the shear layer was ±1.4%. The mean flow has a wake profile until reattachment; after reattachment, the wake flow feature starts to diminish.

The mean velocity vector field in the recirculation region is shown in Fig. 7. A single, clockwise, recirculating bubble was centered above the leading apex of the ramp; in a similar ramp configuration experiment, Petrie et al.[11] found a similar recirculating bubble. Weinberg et al.[7] applied a Navier-Stokes code with an algebraic mixing length turbulence model to a similar ramp configuration with an approach Mach 2.92 flow and a ramp angle of 20 deg and found two clockwise and one counterclockwise recirculating bubbles. It can be seen from Fig. 7 that the recirculating flow was directed toward the

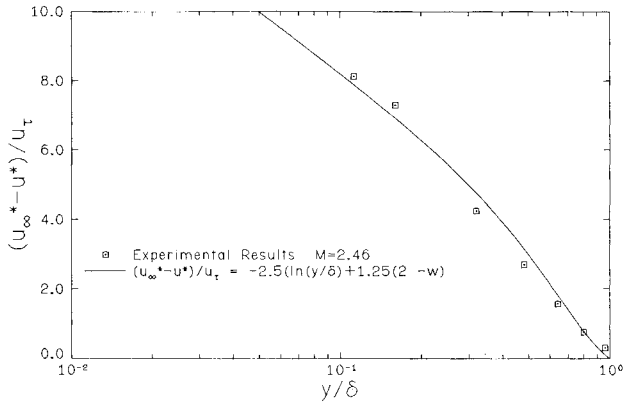

Fig. 2 Boundary-layer mean velocity profile and generalized curve of Maise and McDonald.[21]

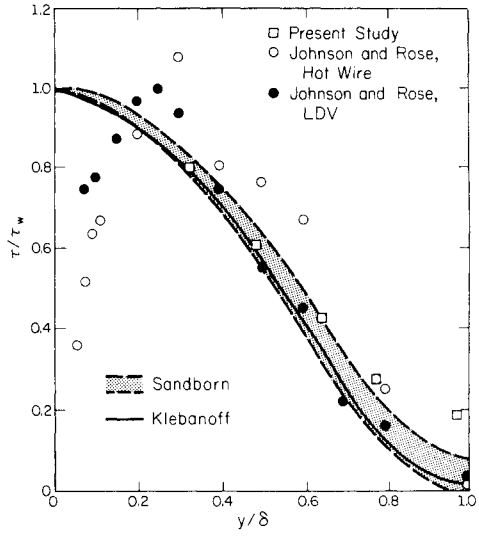

Fig. 3 Boundary-layer shear stress profile.

separation point. This was also noticed by Petrie et al.,[11] but the Navier-Stokes code of Weinberg et al.[7] did not capture this feature of the recirculating bubbles. This feature needs to be studied carefully since it could contribute to the onset of plume-induced flow separation on afterbodies with a centered propulsive jet.

The maximum negative velocity measured in the base region was $0.2u_\infty$, which occurred where the minimum wall pressure was measured. Petrie et al.[11] in a similar experiment, Delery[28] with a transonic freestream and a supersonic propulsive jet, and Etheridge and Kemp[29] in a subsonic flow over a step measured maximum negative velocities of $0.19u_\infty$, $0.30u_\infty$, and $0.18u_\infty$, respectively.

The streamwise mean velocity profiles are shown in a nondimensionalized y coordinate in Fig. 8. The variable δ is the shear or boundary-layer thickness with the classical definition of $\delta = y_{0.99} - y_0$, where y_0, $y_{0.5}$, and $y_{0.99}$ are the locations of $u = 0$, $0.5u_\infty$, and $0.99u_\infty$, respectively. As can be seen from this figure, the collapse of these data is good from two stations after separation up to one station after reattachment. The collapse of these data showed that, in spite of a large adverse pressure gradient, the mean flow in the recompression, reattachment, and initial part of the redeveloping regions is in local equilibrium. It was surprising to see local equilibrium in the reattaching and redeveloping regions under such a large adverse pressure gradient. There are ample experimental results to support the existence of local equilibrium in boundary-layer flows under moderate pressure gradients.[30-32] The similarity parameter, which is used to correlate some overall boundary-layer shape parameter in supersonic flows, is the Clauser pressure gradient coefficient, defined as $(\delta_k^*/\tau_w)(\partial p/\partial x)$, where δ_k^* is the boundary-layer kinematic thickness and τ_w is the wall shear stress. In contrast to the studies cited above, no pressure term was used in the similarity parameter of the present results.

Self-similarity of the mean flow is achieved when the shear layer growth rate becomes linear. A detailed examination of the velocity data and constant velocity lines showed that mean velocity self-similarity was achieved approximately $16\delta_0$ or $200\theta_0$ downstream of the step. Self-similarity in similar experiments by Petrie et al.,[11] Settles et al.,[9] and Ikawa and Kubota[12] were attained at $18.8\delta_0$, $18\delta_0$, and $22\delta_0$ downstream of the step, respectively. The growth rate of the free shear layer was 0.093, which was higher than the values of 0.078 and 0.062 obtained by Petrie et al.[11] and Ikawa and Kubota,[12] respectively, and which was 1.74 times smaller than the incompressible shear layer growth rate of Liepmann and Laufer.[33]

Turbulent Field Results

The streamwise component turbulence intensities are shown in Fig. 9. The x location of each station is given above the profiles. The vertical dashed line at each station shows the local zero. As can be seen, a very pronounced peak turbulence intensity developed just downstream of separation and gradually spread as the shear layer grew. This behavior was also observed by Petrie et al.[11] in supersonic, Delery[28] in transonic, and Driver and Seegmiller[34] in subsonic flows. The peak values increased through recompression and reached a maximum in the reattachment region and decayed afterward. In the recirculating region, the turbulence intensity was high; it was nearly constant at each vertical station and increased in the downstream direction.

The streamwise turbulence intensities nondimensionalized with u_∞ did not collapse onto a single curve as the mean velocity data did in Fig. 8. In Fig. 10 the maximum turbulence intensity at each station was used to nondimensionalize the turbulence intensity data. The turbulence field for $x \geq 30$ mm is locally similar above the sonic line. This was also observed by Petrie et al.[11] in the free shear layer; however, it was sur-

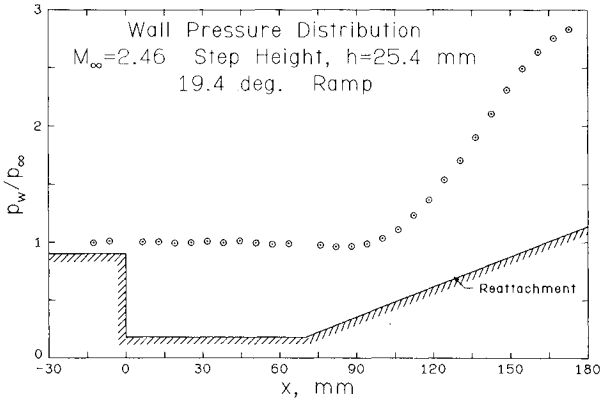

Fig. 4 Streamwise wall static pressure distribution measured on the model centerline.

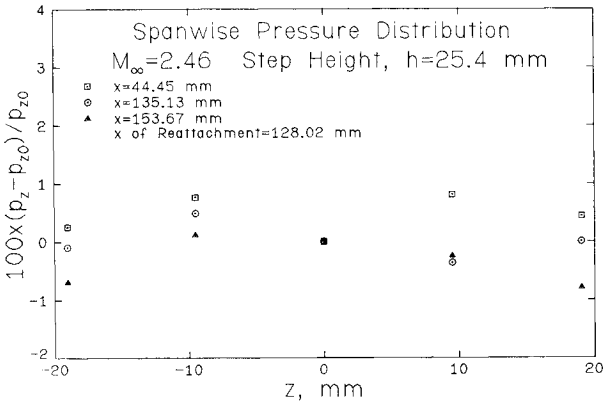

Fig. 5 Spanwise wall pressure distributions.

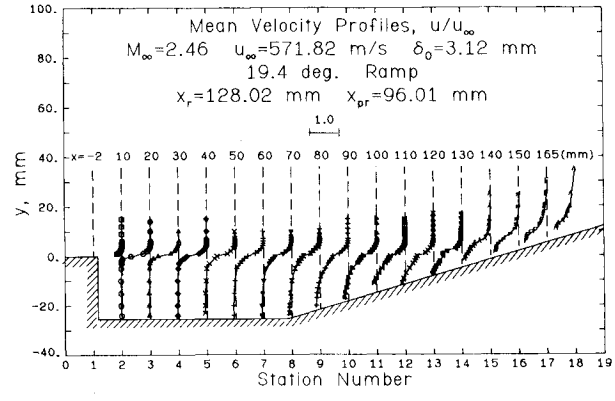

Fig. 6 Streamwise mean velocity profiles.

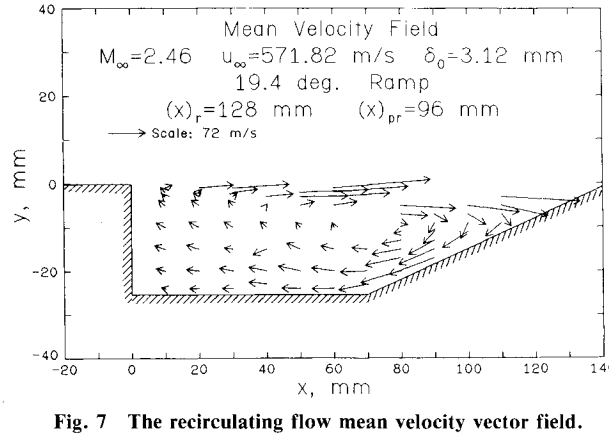

Fig. 7 The recirculating flow mean velocity vector field.

prising to see such local similarity existing in the turbulence field for the reattachment and redevelopment regions under such a large adverse pressure gradient. The maximum turbulence intensities occurred near $y=y_{0.5}$ which was approximately coincident with the sonic line (see Fig. 1). Hayakawa et al.[10] used a hot-wire anemometer for turbulence measurement in a similar geometry, with an incoming Mach 2.92 flow with a turbulent boundary layer. Their results showed that the maximum mass flow fluctuations occurred in the supersonic region of the shear layer. The differences between the present results and Hayakawa's results could be due to the difference between turbulence fluctuation and mass flow fluctuation and/or to difficulties involved in hot-wire calibration for local Mach numbers of 1.2 or less,[10,35] where the maximum intensities occurred during the present study.

The nondimensionalized transverse component turbulence intensities are shown in Fig. 11. In contrast to subsonic shear layers[36,37] the location of the v component maximum turbulence intensities shifted toward the lower velocity side of the mixing layer. The cause of this turbulence behavior change is perhaps the combined effects of compressibility and mean density change across the shear and redeveloping boundary layers. The v component turbulence intensity, nondimensionalized with the maximum turbulence intensity at each station, collapsed above the sonic line as did the streamwise turbulence data.

Evolutionary profiles of the turbulent shear stress are shown in Fig. 12. In the calculation of the mean density $\bar{\rho}$, some interpolations were involved; therefore, at stations 12-17 the mean density is believed to be accurate within $\pm 6.0\%$. As with the u component turbulence intensity, a sharp peak in the shear stress profile developed soon after separation and spread as the shear layer grew. The shear stress increased through recompression, reattachment, and redevelopment of the boundary layer. The maximum shear stress values at each station occurred near the sonic line. The shear stress nondimensionalized with the maximum shear stress at each station collapsed onto a single curve above the sonic line as did the turbulence intensities.

The shear stress fluctuations in the recirculating flow were negligibly small in comparison to the normal stress values (see Fig. 9). The large values of the turbulence intensities and the low values of the shear stress in the recirculating flow could be indicative of a low-frequency flapping motion of the reattaching shear layer. Subsonic flow results[34,38,39] showed relatively high shear stress in the recirculating flow.

The maximum turbulence intensities and shear stresses are shown in Fig. 13. The onset of pressure rise and the reattachment location are identified by *pr* and *r* in Fig. 13. The maximum u and v intensity components reached 15% and 7.5%, respectively, in the constant-pressure shear layer. The ratio of the maximum u intensity to the maximum v intensity in the shear layer region was approximately 1/2, which was similar to that of Petrie et al.[11] but lower than the 2/3 reported for subsonic flows.[37] The maximum u and v component intensities were approximately 22% and 9%, respectively, and both occurred one station after reattachment. The maximum shear stress with the density term increased through recompression and reattachment and reached approximately 0.7% in the redeveloping boundary layer, while the maximum shear stress without the density term leveled off at approximately 0.5% in the reattachment region.

All the experimental results for subsonic shear layer reattachment in the backward-facing step configuration reported in a review paper by Eaton and Johnson[40] showed that the peak values of the maximum u component intensity and maximum shear stress occurred approximately one step height before reattachment followed with a rapid decay. The causes

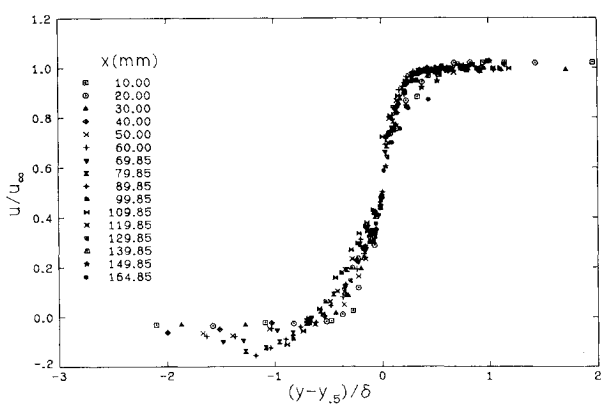

Fig. 8 Correlated streamwise mean velocity profiles.

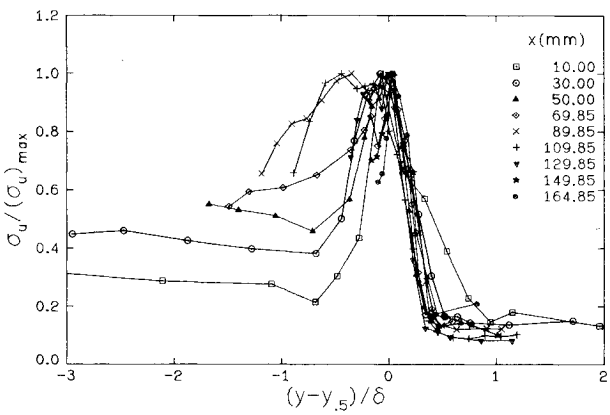

Fig. 10 Correlated streamwise turbulence intensity distributions.

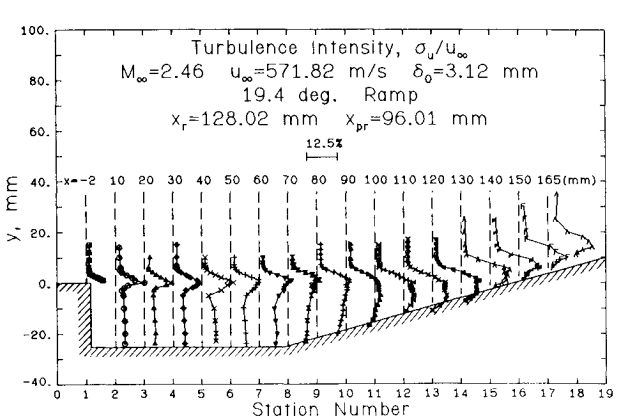

Fig. 9 Streamwise component of the turbulence intensity.

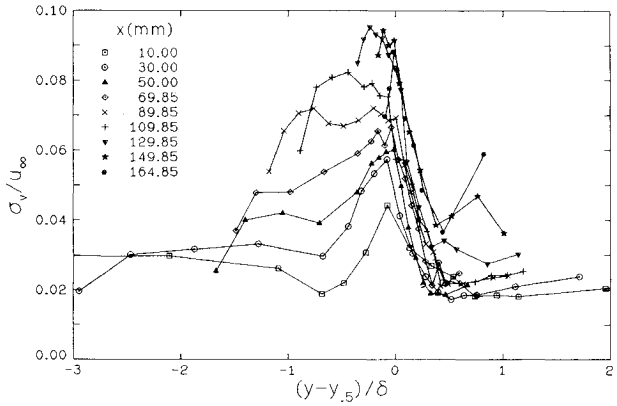

Fig. 11 Correlated transverse component turbulence intensity distributions.

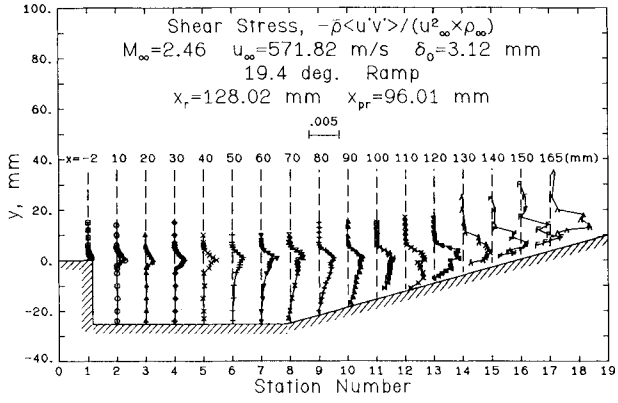

Fig. 12 Turbulent shear stress profiles.

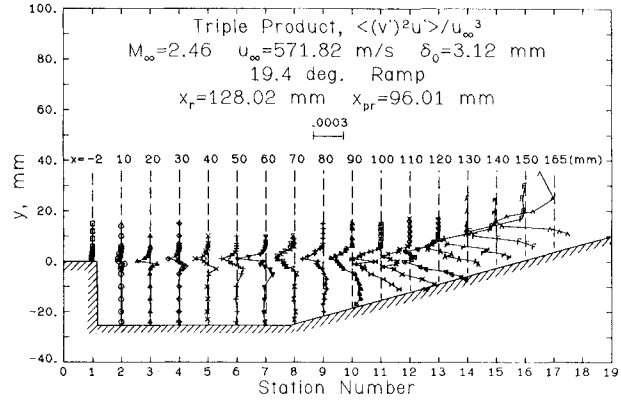

Fig. 14 Turbulent triple product.

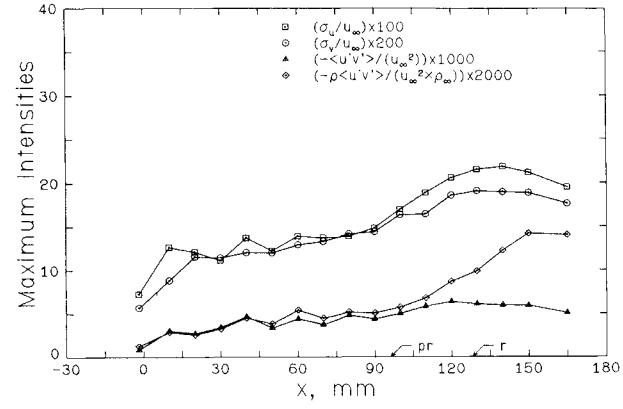

Fig. 13 Maximum turbulence fluctuations and shear stresses.

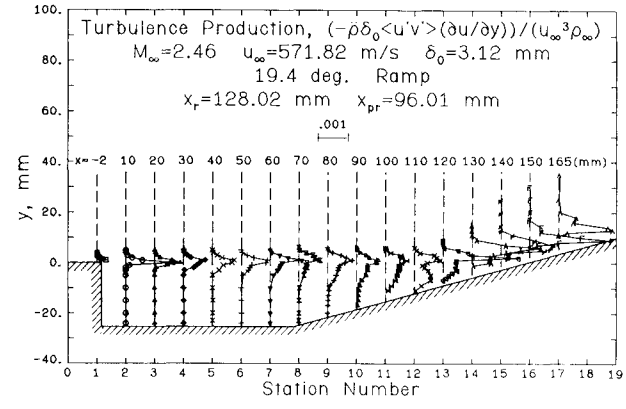

Fig. 15 Turbulence production.

of the rapid decay of turbulence intensity and shear stress for subsonic flows in the reattachment region are not known. The candidate causes are the stabilizing streamline curvature, the adverse pressure gradient, and the strong interaction with the wall.[39,40] Whatever the mechanism(s) for subsonic flow, it seems that compressibility effects are more dominant in supersonic flow reattachment and that there is no turbulence fluctuation decay before or at reattachment.

In turbulence modeling using the turbulent kinetic energy or the shear stress transport equation, one needs to model the turbulent triple products. The evolutionary profiles of one component of the triple products are shown in Fig. 14. As with subsonic plane mixing layers and reattaching shear layers,[34,39] the triple products were observed to be roughly antisymmetrical about the mixing layer center for all four components.[8] The $\langle(u')^3\rangle$ and $\langle u'(v')^2\rangle$ components reached negative minima in the upper portion and positive maxima in the lower portion of the shear layer, which was similar to subsonic shear layers.[34,36,39] The $\langle(u')^2v'\rangle$ and $\langle(v')^3\rangle$ components reached positive maxima in the upper portion and negative minima in the lower portion of the shear layer, which was just the opposite of the subsonic reattaching free shear layers. Therefore, this appears to be another fundamental difference between compressible and incompressible shear layers, which shows the different characteristics of the diffusion of turbulent kinetic energy in the transverse direction in compressible and incompressible shear layers.

As with incompressible reattaching shear layers,[34,39] all four components of the triple products were negligibly small in the recirculating flow. Since the major contributions to triple products come from large-scale turbulence and there is no large-scale motion in the recirculating flow, this was expected. The local values of all four components of the triple products increased dramatically through recompression, reattachment, and redevelopment, which meant large-scale motion and increased length scale in these regions. This behavior was not observed in subsonic flows; rather the triple products on the wall side started decreasing before the reattachment region. Chandrsuda and Bradshaw[39] attributed this behavior to imposition of the $v=0$ condition by the wall and limitation of the large eddies, which are the major contributors to the triple products. Existence of large shear stresses (see Fig. 12) and large triple products could mean large-scale motion and large turbulence length scales in the redeveloping boundary layer.

Turbulence production plays an important role in the streamwise evolution of separated flowfields. The component of turbulence production that could be obtained experimentally with reasonable accuracy was the production by shear stresses, $Pr=-\bar{\rho}\langle u'v'\rangle\partial u/\partial y$. The turbulence production profiles developed a peak soon after separation and spread as the shear layer grew (see Fig. 15). The peak value at each station was located around the sonic line and reached a maximum near the reattachment region and started decaying afterward.

Conclusions

A detailed experimental study of reattaching compressible, turbulent, free shear layers using LDV techniques was carried out. Local similarity of the mean flow was observed through the shear layer, the reattachment, and the initial part of the redeveloping boundary layer. The mean flow and the turbulence field above the sonic line correlated with the local shear or the local boundary-layer thickness. The growth rate of the shear layer was 1.74 times less than that of incompressible shear layer. In contrast to incompressible reattaching shear layers, the turbulence intensities, shear stress, and turbulent triple products were significantly increased through reattachment. Existence of large turbulent triple products and large shear stress in the recompression, reattachment, and

redevelopment regions indicated the presence of a large-scale turbulence field in these regions. Evolution of the turbulence field in reattaching compressible shear layers seems to be very complex and offers a great challenge to turbulence modelers. Probably models based on the shear stress transport equation with relatively sophisticated models for the turbulent triple products are required.

Acknowledgment

This research was supported by the U.S. Army Research Office. Dr. Robert E. Singleton served as the Contractor Monitor.

References

[1]Chapman, D. R., "An Analysis of Base Pressure at Supersonic Velocities and Comparison with Experiment," NACA TN 2137, 1950.

[2]Korst, H. H., "A Theory for Base Pressures in Transonic and Supersonic Flow," *Journal of Applied Mechanics*, Dec. 1956, pp. 593-600.

[3]Less, L. and Reeves, B. L., "Supersonic Separated and Reattaching Laminar Flows: I. General Theory and Application to Adiabatic Boundary Layer/Shock Wave Interactions," *AIAA Journal*, Vol. 2, Feb. 1964. pp. 1907-1920.

[4]Alber, I. E. and Less, L., "Integral Theory for Supersonic Turbulent Base Flows," *AIAA Journal*, Vol. 6, July 1968, pp. 1343-1351.

[5]Marvin, J. G., "Turbulence Modeling for Computational/Aerodynamics," AIAA Paper 82-0164, Jan. 1982.

[6]Horstmann, C. C., Settles, G. S., Bogdonoff, S. M., and Williams, D. R., "A Reattaching Free Shear Layer in Compressible Turbulent Flow—A Comparison of Numerical and Experimental Results," *AIAA Journal*, Vol. 20, Jan. 1982, pp. 79-85.

[7]Weinberg, B. C., McDonald, H., and Shamroth, S. J., "Navier-Stokes Computations of Aft End Flow Fields," Final Report, U.S. Army Research Office Contract DAAG 29-79-C-0003, Scientific Research Associates, Inc., Glastonbury, CT, May 1982.

[8]Samimy, M., "An Experimental Study of Compressible Turbulent Reattaching Free Shear Layers," Ph.D. Thesis, Dept. of Mechanical and Industrial Engineering, Univ. of Illinois at Urbana-Champaign, 1984.

[9]Settles, G. S., Baca, B. K., Williams, D. R., and Bogdonoff, S. M., "A Study of Reattachment of a Free Shear Layer in Compressible, Turbulent Flow," AIAA Paper 80-1408, 1980; also, *AIAA Journal*, Vol. 20, Jan. 1982, pp. 60-67.

[10]Hayakawa, K., Smiths, A. J., and Bogdonoff, S. M., "Turbulence Measurements in a Compressible Reattaching Shear Layer," AIAA Paper 83-0299, Jan. 1983.

[11]Petrie, H. L., Samimy, M., and Addy, A. L., "A Study of Compressible Turbulent Free Shear Layers Using Laser Doppler Velocimetry," AIAA Paper 85-0177, Jan. 1985.

[12]Ikawa, H. and Kubota, T., "Investigation of Supersonic Turbulent Mixing Layer with Zero Pressure Gradient," *AIAA Journal*, Vol. 13, March 1975, pp. 566-572.

[13]Buchhave, P., "Biasing Errors in Individual Particle Measurements with the LDA-Counter Signal Processor," *Proceedings of LDV Symposium*, Copenhagen, Denmark, 1975, pp. 258-278.

[14]Dimotakis, P. E., "Single Scattering Particle Laser Doppler Measurements of Turbulence," AGARD-CP-193, 1976, pp. 10-1 to 10-14.

[15]Whiffen, M. C., "Polar Response of an LV Measurement Volume," *Proceedings of the Minnesota Symposium on Laser Velocimetry*, Univ. of Minnesota, Minneapolis, 1975, pp. 589-590.

[16]Petrie, H. L., "A Study of Compressible Turbulent Free Shear Layers Using Laser Doppler Velocimetry," Ph.D. Thesis, Dept. of Mechanical and Industrial Engineering, Univ. of Illinois at Urbana-Champaign, 1984.

[17]Erdmann, J. C. and Tropea, C., "Turbulent Induced Statistical Bias in Laser Anemometry," *Proceedings of the Seventh Symposium on Turbulence*, Univ. of Missouri-Rolla, Sept. 1981, pp. 129-138.

[18]Erdmann, J. C. and Tropea, C., "Statistical Bias of the Velocity Distribution Function in Laser Anemometry," Paper 16.2, International Symposium on Applications of Laser Doppler Anemometry to Fluid Mechanics, Lisbon, Portugal, July 1982.

[19]Kried, D. K., "Laser-Doppler Velocimeter Measurements in Nonuniform Flow: Error Estimates," *Applied Optics*, Vol. 13, Aug. 1974, pp. 1872-1881.

[20]Karpuk, M. E. and Tiederman, W. G., "Effect of Finite-Size Probe Volume Upon Laser Doppler Anemometer Measurements," *AIAA Journal*, Vol. 14, Aug. 1976, pp. 1099-1105.

[21]Maise, G. and McDonald, H., "Mixing Length and Kinematic Eddy Viscosity in a Compressible Boundary Layer," *AIAA Journal*, Vol. 6, Jan. 1968, pp. 73-80.

[22]Klebanoff, D. S., "Characteristics of Turbulence in a Boundary Layer with Zero Pressure Gradient," NACA Rept. 1247, 1955.

[23]Sandborn, V. A., "A Review of Turbulence Measurements in Compressible Flow," NASA TM X-62, March 1974.

[24]Johnson, D. A. and Rose, W. C., "Laser Velocimeter and Hot-Wire Anemometer Comparison in a Supersonic Boundary Layer," *AIAA Journal*, Vol. 13, April 1975, pp. 512-515.

[25]Roshko, A. and Thomke, G. J., "Observations of Turbulent Reattachment Behind an Axisymmetric, Downstream-Facing Step in Supersonic Flow," *AIAA Journal*, Vol. 4, June 1966, pp. 975-980.

[26]Sirieix, M., Mirande, J., and Delery, J., "Expériences Fondamentales sur le Recollement Turbulent d'un Jet Supersonique," NATO AGARD CP No. 4, Pt. I, 1966, pp. 353-391.

[27]Inger, G. R., "Three-Dimensional Heat- and Mass-Transfer Effects across High-Speed Reattaching Flows," *AIAA Journal*, Vol. 15, March 1977, pp. 383-389.

[28]Delery, J. M., "ONERA Research on Afterbody Viscid/Inviscid Interaction with Special Emphasis on Base Flows," *Proceedings of the Symposium on Rocket/Plume Fluid Dynamic Interactions*, Huntsville, AL, April 1983, Bertin, J., (ed.), University of Texas at Austin, Rept. 83-104.

[29]Etheridge, D. W. and Kemp, P. H., "Measurements of Turbulent Flow Downstream of a Rearward-Facing Step," *Journal of Fluid Mechanics*, Vol. 86, Pt. 3, June, 1978, pp. 545-566.

[30]Laderman, A. J., "Adverse Pressure Gradient Effect on Supersonic Boundary Layer Turbulence," *AIAA Journal*, Vol. 18, Oct. 1980, pp. 1186-1195.

[31]Lewis, J. E., Gran, R. L., and Kubota, T., "An Experiment on the Adiabatic Compressible Turbulent Boundary Layer in Adverse and Favorable Pressure Gradients," *Journal of Fluid Mechanics*, Vol. 51, Pt. 4, Feb. 1972, pp. 657-672.

[32]Coles, D., "Remarks on Equilibrium Turbulent Boundary Layers," *Journal of the Aeronautical Sciences*, Vo. 24, 1957, pp. 495-506.

[33]Liepmann, H. W. and Laufer, J., "Investigation of Free Turbulent Mixing," NACA TN 1257, 1947.

[34]Driver, D. M. and Seegmiller, H. L., "Features of Reattaching Turbulent Shear Layer Subject to an Adverse Pressure Gradient," AIAA Paper 82-1029, 1982.

[35]Kovasznay, L. S. G., "The Hot-Wire Anemometer in Supersonic Flow," *Journal of the Aeronautical Sciences*, Vol. 71, Pt. 4, 1950, pp. 565-573.

[36]Wygnanski, I. and Fiedler, H. E., "The Two-Dimensional Mixing Region," *Journal of Fluid Mechanics*, Vol. 41, Pt. 2, April 1970, pp. 327-361.

[37]Champagne, F. H., Pao, Y. H., and Wygnanski, I. J., "On the Two-Dimensional Mixing Region," *Journal of Fluid Mechanics*, Vol. 74, Pt. 2, 1976, pp. 209-250.

[38]Bradshaw, P. and Wong, F. Y. F., "The Reattachment and Relaxation of Turbulent Shear Layer," *Journal of Fluid Mechanics*, Vol. 52, Pt. I, 1972, pp. 113-135.

[39]Chandrsuda, C. and Bradshaw, P., "Turbulence Structure of a Reattaching Mixing Layer," *Journal of Fluid Mechanics*, Vol. 110, Sept. 1981, pp. 171-194.

[40]Eaton, J. K. and Johnston, J. P., "A Review of Research on Subsonic Turbulent Flow Reattachment," *AIAA Journal*, Vol. 19, Sept. 1981, pp. 1093-1100.